Journal of Hazardous Materials 186 (2011) 1541–1552

Contents lists available at ScienceDirect

Journal of Hazardous Materials

journal homepage: www.elsevier.com/locate/jhazmat

Bioaccumulation of the synthetic dye Basic Violet 3 and heavy metals in single and binary systems by *Candida tropicalis* grown in a sugarcane bagasse extract medium: Modelling optimal conditions using response surface methodology (RSM) and inhibition kinetics

Devlina Das, D. Charumathi, Nilanjana Das*

Environmental Biotechnology Division, School of Biosciences and Technology, VIT University, Vellore 632 014, Tamil Nadu, India

ARTICLE INFO

Article history:
Received 17 September 2010
Received in revised form 8 December 2010
Accepted 8 December 2010
Available online 15 December 2010

Keywords:
Basic Violet 3
C. tropicalis
Bioaccumulation
Heavy metals
Response surface methodology

ABSTRACT

Single and binary effects of dye Basic Violet 3 and heavy metals, 'namely', Pb(II) and Cd(II), were investigated for their role in dye and heavy metal bioaccumulation by *Candida tropicalis* that was grown in a sugarcane bagasse extract medium containing 8 g/L, 16 g/L or 24 g/L of sugar. The optimum pH was found to be 4.0 in the single system and 5.0 in the binary system. A central composite design was successfully used to analyse the experimental results. Four numerical correlations that were fitted to a second order quadratic equation were used to estimate optimum combinations predicted by response surface methodology. In the dye–Pb(II) binary system, *C. tropicalis* was capable of bioaccumulating 49.5% of the dye and 49.6% of the Pb(II), in comparison to 15.9% of the dye and 55.5% of the Cd(II) in the dye–Cd(II) binary system. In these two systems, the pollutants were dispersed at minimum working concentration levels. Competitive inhibition was observed in both the single and binary systems, which was suggested by an increase in the saturation constant, K_s, and a simultaneous decrease in the specific growth rate that was calculated from Lineweaver–Burk plots. Atomic force microscopy images demonstrated changes in yeast cell morphology by exposure to these contaminants in the dye–Pb(II) binary system grown in a bioaccumulation medium.

1. Introduction

Synthetic dyes are commonly used in textile, tannery, pharmaceutical, paper, paint, plastics, electroplating and cosmetics industries [1]. Heavy metals are sometimes added to stabilise the colour of these dyes and to enhance the binding of the dye to the fibre. As a result, wastewater generated from these industries can contain dye and heavy metal ions bound together [2]. Both the dyes and heavy metals can be toxic and mutagenic when they are discharged directly into the environment. Although some physicochemical methods have been developed for effective dye removal, they are often limited by their cost, regeneration efficiency, emission of secondary pollutants, limited versatility, interactions with other wastewater constituents and residual sludge generation [3]. Heavy metals can be removed from industrial wastewater by conventional methods, viz., chemical precipitation, chemical oxidation and reduction, ion exchange, filtration, adsorption and evaporation, but the regulatory standards for their elimination are not always sufficient [4]. Biological processes such as biosorption [5,6] and bioaccumulation [7,8] have been proposed as potential alternative methods for the removal of heavy metals from wastewater.

The bioaccumulation of dyes has received a great deal of attention in recent years, not only as a scientific novelty but also for its potential application in industry. Some reports have discussed the feasibility of using growing yeast cells for the bioaccumulation of dyes [9–11] as well as for the bioaccumulation of heavy metals [7,8] in a single system. However, these data do not address an environment in which wastewater contains both dye and heavy metals. In these situations, bioaccumulation not only depends on the biomass and physicochemical parameters, such as pH and temperature, but it also depends on the number of metal species and their concentrations [12–15]. Therefore, it is important to understand how the bioaccumulation properties of living organisms are altered by competitive or cooperative effects in the environment as well as the mechanisms of these processes to accurately predict the bioaccumulation behaviours of contaminants in a mixed system.

Response surface methodology (RSM) combines mathematical and statistical techniques used for developing, improving and optimizing processes, and it is used to evaluate the relative significance of several important factors, even in the presence of complex inter-

* Corresponding author. Tel.: +91 416 2202478; fax: +91 416 2243092.
E-mail address: nilanjana00@lycos.com (N. Das).

0304-3894/$ – see front matter © 2010 Elsevier B.V. All rights reserved.
doi:10.1016/j.jhazmat.2010.12.038

actions. Although RSM has been used to optimise parameters, viz., pH, pollutant concentration and bioaccumulation of metals [16,17] and dyes from synthetic solutions [18], few studies have addressed optimizing the dye and heavy metal components in media for the simultaneous removal of both of these components.

Therefore, in this study, we investigated the bioaccumulation of synthetic dye Basic Violet 3 and heavy metals that are frequently found in wastewater, viz., Pb(II) and Cd(II), in single and binary systems using *Candida tropicalis* grown in a sugarcane bagasse extract medium at batch scale. Functional relationships between dye removal and heavy metal removal in the binary systems were determined using RSM. The use of sugarcane bagasse extract, an inexpensive waste product, as a nutrient source is one of the attractive features of this study. Mathematical models of competitive, uncompetitive and non-competitive inhibition have been proposed to describe the inhibitory effects of the dye and the heavy metals on *C. tropicalis* bioaccumulation. The aim of this research was to investigate the bioaccumulation properties of *C. tropicalis* for preferential uptake of dye and Pb(II) and Cd(II) ions in single and binary systems.

2. Materials and methods

2.1. Dye and heavy metal solutions

Basic Violet 3 is a cationic dye commonly used in textile industries. It was obtained in pure form from Manisha Textile dyeing works, Kanchipuram, Tamil Nadu, India. The dye stock solution (100 mg/L) was prepared by dissolving 0.1 g of powdered dyestuff in 1000 mL of deionised water. The working solutions of dye were prepared by diluting the stock solution to the desired concentration. The working solutions of heavy metals, Pb(II) and Cd(II), were prepared by diluting stock solutions from Merck Pvt Ltd., UK.

2.2. Microorganisms and growth media

C. tropicalis cells were isolated from dye-contaminated sludge that was collected from a textile dyeing industry, Kanchipuram, Tamil Nadu, India. The yeast was phenotypically characterised and identified to a species level by VITEK 2 Compact Yeast card reader with software version V2C 1.01 at the Council for Food Research and Development (CFRD), Kerala, India. The isolate was maintained in yeast extract peptone dextrose (YEPD) agar slants. Because *C. tropicalis* could not use the dye as its sole carbon source for the cell growth, an aqueous extract of sugarcane bagasse was chosen as the growth medium, and it was prepared as reported in our previous study [19]. The yeast species was first grown in a mineral medium composed of glucose (10 g), KH_2PO_4 (1 g), $(NH_4)_2SO_4$ (1 g), $MgSO_4{\cdot}7H_2O$ (500 mg), yeast extract (200 mg) and deionised water (1 L). The pH of the medium was adjusted to 5.0 with HCl (0.1 N) and NaOH (0.1 N). The preculture was incubated on a rotary shaker at 120 rpm and at a temperature of 28 °C. To prepare the bioaccumulation medium, dye and heavy metals were autoclaved separately and the mixed with a sterilised aqueous extract of sugarcane bagasse.

2.3. Bioaccumulation assays

We investigated the effects of the initial pH on dye and heavy metal bioaccumulation in single and binary systems by varying the pH of the growth medium from 3 to 7. The effects of the initial concentration levels of the dye and heavy metals on bioaccumulation were also investigated in single and binary systems by varying the dye concentration from 10 to 50 mg/L and varying the concentration of heavy metals from 2 to 10 mg/L in the bioaccumulation medium. An aliquot of the preculture (2 mL) was harvested during its exponential growth phase, and it was transferred to the bioaccumulation medium (50 mL) supplemented with dye at 10–50 mg/L and heavy metals at 2–10 mg/L. The cultures were grown at 28 °C on a rotary shaker at 120 rpm for 2 days.

2.4. Analytical methods

During the incubation period, 2 mL samples were taken from each flask at regular time intervals. The aliquots were centrifuged at 10,000 rpm for 5 min, and the supernatant fractions were collected to measure heavy metal and dye concentration levels. The residual heavy metal concentration levels were measured on an atomic absorption spectrophotometer (Varian AA 240, Australia). The residual dye concentration levels were determined by UV–vis spectroscopy at 584 nm (HITACHI U-2800, Japan). The cells were washed after centrifugation and dried at 40 °C to measure the dry cell mass concentration. The bioaccumulation % of dye and heavy metals was calculated using the following equation:

$$\text{Bioaccumulation\%} = \frac{C_0 - C_f}{C_f} \times 100 \quad (1)$$

where C_0 is the initial concentration of dye or metal (mg/L) and C_f is the final concentration of dye or metal (mg/L).

2.5. Statistical analysis

In multivariable systems, the classical approach of changing one variable at a time to study the effects on other variables for a particular response is time consuming. Therefore, an alternate strategy involving statistical approaches, e.g., response surface methodology (RSM), was applied to solve for multiple variables in this complex system. The need to ensure the effectiveness of the biological wastewater treatment using growing cells has stimulated the use of mathematical models for predicting microbial behaviour. The objective of the this study was not only to investigate the combined effects of Basic Violet 3 and heavy metal concentration levels on bioaccumulation properties of yeast but also to find the best model equations to simultaneously represent both dye and heavy metals, viz., Pb(II) and Cd(II).

In the optimization procedure we studied the response of the statistically designed combinations, estimated the coefficients by fitting the experimental data to the response functions, predicted the response of the fitted model and checked the adequacy of the model. The complete design consisted of 13 runs, each of which was performed in duplicate. The statistical software Design Expert® was used for numerical analysis and to estimate the responses of dye and Pb(II) as well as dye and Cd(II). The statistical significance of the model equation and the goodness of fit were evaluated by R^2 and by the *F*-test analysis of variance (ANOVA), which is a statistical technique that subdivides the total variation in a set of data into components associated with specific sources of variation to test hypotheses on the parameters of the model. A large *F*-value indicates that most of the variation can be explained by a regression equation, whereas a low *p*-value (<0.05) indicates that the model is considered to be statistically significant [16–18,20].

2.6. Kinetic approach

The relationship between the specific growth rate and substrate concentration in the absence of inhibitory substances, such as dyes, is described by the Monod equation given below:

$$\mu = \frac{\mu_m}{1 + (K_s/S)} \quad (2)$$

where S is the substrate concentration (g/L), μ and μ_m are the specific growth rate and the maximum specific growth rate of the

microorganism (h^{-1}), respectively, and K_s is the saturation constant (g/L). Eq. (2) can be linearised in the following double-reciprocal form:

$$\frac{1}{\mu} = \frac{1}{\mu_m} + \frac{K_s}{\mu_m}\frac{1}{S} \quad (3)$$

K_s and μ_m values can be determined from the plot of $1/\mu$ versus $1/S_0$ (assuming $S = S_0$ at the beginning of exponential growth), which yields a linear line with a slope of K_s/μ_m and y-axis intercept of $1/\mu_m$. In presence of inhibitory (toxic) substances, such as dyes in nutrient media, microbial growth becomes inhibited, and the specific growth rate depends on the concentration of the inhibitor. Inhibition models, viz., competitive, non-competitive and uncompetitive, are classified according to the effect of toxic compounds on the specific growth rate and saturation constant. The rate equations for these models are described in the following sections [21,22].

2.6.1. Competitive inhibition

Competitive inhibitors compete with the substrate and each other to bind to active sites on microorganism cells.

Assuming rapid equilibrium, the following equation was developed to describe the specific growth rate of the microorganism if n inhibitors compete with substrate in the growth medium;

$$\mu = \frac{\mu_m S}{K_s\left[1 + \sum_{i=1}^{n}(I_i/K_{Ii})\right] + S} \quad (4)$$

where I is the concentration of the component that causes inhibition (mg/L) and K_I is the inhibition constant (mg/L). Competitive inhibition causes an increased value of the apparent saturation constant ($K'_{s,app}$) is described in the following equation:

$$K'_{s,app} = K_s\left[1 + \sum_{i=1}^{n}\frac{I_i}{K_{Ii}}\right] \quad (5)$$

Therefore, competitive inhibition leads to a reduction in the specific growth rate.

2.6.2. Non-competitive inhibition

Non-competitive inhibitors bind to sites other than the active site and reduce microorganism affinity for the substrate. The following equation describes the specific growth rate of the microorganism if non-competitive inhibitors are present in the growth medium:

$$\mu = \frac{\mu_m S}{(K_s + S)\left[1 + \sum_{i=1}^{n}(I_i/K_{Ii})\right]} \quad (6)$$

Non-competitive inhibition causes a reduction in the maximum specific growth rate.

2.6.3. Uncompetitive inhibition

Uncompetitive inhibitors bind to the microorganism–substrate (MS) complex only and have no affinity for the microorganism itself. The following equation describes the specific growth rate of the microorganism if uncompetitive inhibitors are present in the growth medium:

$$\mu = \frac{\mu_m S}{K_s + S\left[1 + \sum_{i=1}^{n}(I_i/K_{Ii})\right]} \quad (7)$$

where uncompetitive inhibition causes a reduction in both the maximum specific growth rate, and $K'_{s,app}$.

2.7. Preparation of AFM samples

The yeast cells were prepared before and after their bioaccumulation of dye and Pb(II) in a medium containing 50 mg/L of dye and 10 mg/L of Pb(II) in a single system and a binary system. Cells were suspended in sterilised deionised water and fixed on a cover glass. The surface morphology of the yeast cells was observed using an atomic force microscope (AFM) (Nanosurf easyscan 2, Netherlands).

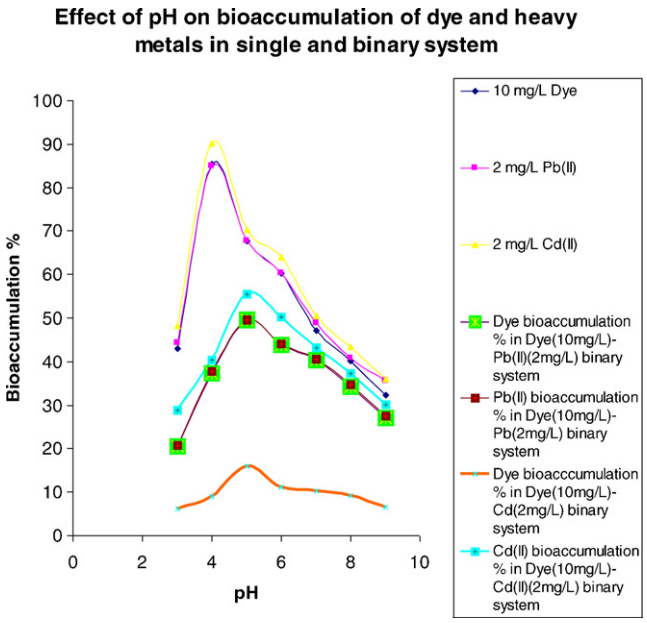

Fig. 1. Effect of pH on bioaccumulation of dye and heavy metals in single and binary system by *C. tropicalis*.

3. Results and discussion

3.1. Effect of pH on the bioaccumulation of dye and heavy metals in single and binary systems

The effect of pH on the bioaccumulation of dye and heavy metals, viz., Pb(II) and Cd(II), in single and binary systems by *C. tropicalis* was investigated by varying the pH of the growth medium from 3.0 to 7.0 (Fig. 1). The bioaccumulation of dye and metal cations, viz., Pb(II) and Cd(II), by yeast increased with increasing pH values up to 4.0. Aksu and Donmez [23] also reported maximum bioaccumulation levels for Cu(II) by *C. tropicalis* at pH 4.0. Similar results were reported by Gonen and Aksu [24]. In the binary system, the percentages of bioaccumulation of the dye and heavy metals were maximised at pH 5.0 (Fig. 1). Increasing the pH values increased the negative charges on the yeast cell surface, thereby favouring the bioaccumulation of cationic dye Basic Violet 3 and the metal cations, viz., Pb(II) and Cd(II), in both the single and binary systems.

3.2. Bioaccumulation of Basic Violet 3, Pb(II) and Cd(II) in a single system

In a single system, the bioaccumulation of Basic Violet 3, Pb(II) and Cd(II) by *C. tropicalis* was investigated at the empirically optimal pH of 4.0 in a sugarcane bagasse extract medium. The percentage of bioaccumulation and corresponding biomass and specific growth rate are presented in Table 1. The amount of bioaccumulated dye increased up to 50 mg/L, while the biomass and specific growth rate exhibited a decreasing trend, indicating that media toxicity increased with increasing dye concentration. In the presence of 10 mg/L of dye, the bioaccumulation % was 85.3%, which was reduced to 53.9% at 50 mg/L of dye. Furthermore, biomass decreased from 2.11 g/L to 0.83 g/L, and the specific growth rate decreased from 0.247 to 0.226 h^{-1}. Changing the concentration

Table 1
Comparison of Basic Violet 3 and Pb(II) bioaccumulation, biomass (X_m), specific growth rate (μ) at different levels of dye and Pb(II) concentration for single and binary system.

C_{0BV} (mg/L)	C_{0PbII} (mg/L)	B.V. accumulation (%)	Pb(II) accumulation (%)	B.V. conc. (mg/L)	Pb(II) conc. (mg/L)	X_m (g/L)	μ (h^{-1})
10	0	85.3	0	8.53	0	2.11	0.247
20	0	72.5	0	14.5	0	1.72	0.242
30	0	65.0	0	19.5	0	1.43	0.234
40	0	57.1	0	22.8	0	1.11	0.229
50	0	53.9	0	26.9	0	0.83	0.226
0	2	0	85.0	0	1.70	2.00	0.246
0	4	0	72.3	0	2.89	1.72	0.242
0	6	0	65.0	0	3.90	1.42	0.233
0	8	0	57.0	0	4.56	1.11	0.229
0	10	0	53.7	0	5.37	0.83	0.226
10	2	49.5	49.6	4.95	0.992	1.54	0.187
20	2	42.1	42.2	8.42	0.84	1.42	0.173
30	2	35.9	36.1	10.77	0.72	1.34	0.164
40	2	27.7	27.8	11.08	0.56	1.27	0.155
50	2	16.8	17.6	8.4	0.352	1.14	0.137
10	4	45.0	45.5	4.5	1.82	1.24	0.151
20	4	40.1	40.9	8.02	1.64	1.17	0.142
30	4	33.3	33.5	9.99	1.34	1.02	0.119
40	4	25.9	26.1	10.36	1.04	0.90	0.098
50	4	14.6	15.1	7.3	0.60	0.81	0.080
10	6	40.1	40.60	4.01	2.44	1.07	0.127
20	6	34.0	34.30	6.80	2.06	0.93	0.103
30	6	23.0	23.20	6.90	1.36	0.82	0.082
40	6	20.6	20.90	8.24	1.25	0.74	0.065
50	6	13.2	13.30	6.60	0.79	0.63	0.039
10	8	35.7	35.8	3.57	2.86	0.94	0.105
20	8	30.2	30.6	6.04	2.45	0.82	0.082
30	8	31.1	31.3	6.33	1.70	0.71	0.058
40	8	16.3	16.7	6.52	1.34	0.62	0.036
50	8	12.2	12.5	6.10	1.00	0.54	0.013
10	10	14.1	13.9	1.41	1.39	0.82	0.082
20	10	14.0	13.5	1.28	1.35	0.74	0.065
30	10	13.8	13.2	4.14	1.32	0.61	0.033
40	10	13.7	13.1	5.50	1.31	0.53	0.009
50	10	10.8	10.9	5.40	1.09	0.51	0.003

from 10 to 50 mg/L resulted in increased bioaccumulation levels from 8.53 mg/L to 26.9 mg/L. A similar trend in bioaccumulation levels of RTBG dye and Cu(II) by *C. tropicalis* was also observed by Gonen and Aksu [25].

Increasing the concentration of heavy metals, viz., Pb(II) and Cd(II), also led to reduced bioaccumulation %, biomass and specific growth rate. The bioaccumulation % decreased from 85% to 53.7% when the concentration of Pb(II) increased from 2 mg/L to 10 mg/L. This result was supported by a reduction in the specific growth rate from 0.246 to 0.226 h^{-1}.

A similar trend was observed for bioaccumulation in the Cd(II) system (Table 2). A higher bioaccumulation % of 90.1% was observed at 2 mg/L, which decreased to 57.6 mg/L at a metal concentration of 10 mg/L. A decrease in biomass from 2.90 g/L to 2.50 g/L was also observed as the Cd(II) concentration was increased. These results suggest that Basic Violet 3 and Pb(II) exhibit similar trends in bioaccumulation, biomass and specific growth rate, whereas Cd(II) exhibited a higher bioaccumulation, biomass and specific growth rate at all concentrations. Thus the data demonstrate that in a single system, the dye and Pb(II) exhibit similar toxicity levels, whereas Cd(II) exhibited lower toxicity compared to other two pollutants.

3.3. Bioaccumulation of Basic Violet 3 and Pb(II) in a binary system

In the binary system, both Basic Violet 3 and Pb(II) bioaccumulation % were reduced to a similar extent when the concentration of the dye was increased at a fixed Pb(II) concentration. This result indicates that Basic Violet 3 and Pb(II) were equally bioaccumulated by *C. tropicalis*, thereby suggesting that they exhibit a similar degree of competition for the sites on the *C. tropicalis* cell wall (Table 1). At their minimum concentration levels, the maximum amount of bioaccumulation for Basic Violet 3 (at 10 mg/L) and Pb(II) (at 2 mg/L) was 49.5% and 49.6%, respectively. Basic Violet 3 bioaccumulation increased up to 40 mg/L at every Pb(II) concentration that was tested except for at 50 mg/L, for which it exhibited decreased bioaccumulation. This increase in bioaccumulation was likely a result of the increased initial dye concentration, but at 50 mg/L of initial dye concentration, the toxicity of the dye likely hindered further bioaccumulation. At the minimum concentration levels of Pb(II) and dye, the biomass was 1.54 g/L and the specific growth rate was 0.187 h^{-1} (Table 1). The maximum decrease in biomass was 0.51 g/L, and the maximum decrease in specific growth rate was 0.003 h^{-1}, during which both toxic components were at their maximum concentration levels. In the presence of Pb(II), the dye bioaccumulation changed to a similar extent as did the bioaccumulation of Pb(II) in the presence of dye.

3.4. Bioaccumulation of Basic Violet 3 and Cd(II) in a binary system

Data shown in Table 2 demonstrate that increasing the concentration of dye at a fixed Cd(II) concentration resulted in a larger decrease in the bioaccumulation % of the dye compared to Cd(II). This result indicated that the dye bioaccumulation was a function of the initial Cd(II) concentration.

The maximum amount of bioaccumulation for Basic Violet 3 and Cd(II) was 15.9% and 55.5%, respectively, for initial concentration

Table 2
Comparison of Basic Violet 3 and Cd(II) bioaccumulation, biomass (X_m), specific growth rate (μ) at different levels of dye and Cd(II) concentration for single and binary system.

C_{0BV} (mg/L)	C_{0CdII} (mg/L)	B.V. accumulation (%)	Cd(II) accumulation (%)	B.V. conc. (mg/L)	Cd(II) conc. (mg/L)	X_m (g/L)	μ (h^{-1})
10	0	85.3	0	8. 53	0	2.11	0.247
20	0	72.5	0	14.5	0	1.72	0.242
30	0	65.0	0	19.5	0	1.43	0.234
40	0	57.1	0	22.8	0	1.11	0.229
50	0	53.9	0	26.9	0	0.83	0.226
0	2	0	90.1	0	1.80	2.90	0.251
0	4	0	81.5	0	3.26	2.80	0.246
0	6	0	70.1	0	4.21	2.69	0.240
0	8	0	61.3	0	4.90	2.58	0.234
0	10	0	57.6	0	5.76	2.50	0.229
10	2	15.9	55.5	1.59	1.10	1.97	0.228
20	2	13.2	49.8	2.64	0.99	1.90	0.222
30	2	12.6	36.5	3.78	0.73	1.84	0.217
40	2	10.9	20.6	4.36	0.412	1.74	0.208
50	2	4.4	15.4	2.20	0.308	1.62	0.196
10	4	14.3	50.10	1.43	2.00	1.83	0.216
20	4	13.0	45.3	2.60	1.81	1.79	0.212
30	4	12.4	32.1	3.72	1.28	1.69	0.203
40	4	10.1	17.30	4.04	0.69	1.61	0.195
50	4	3.9	13.3	1.95	0.53	1.54	0.187
10	6	13.1	41.30	1.31	2.48	1.76	0.209
20	6	12.1	39.90	2.42	2.39	1.64	0.198
30	6	10.2	20.50	3.06	1.23	1.58	0.192
40	6	8.5	13.60	3.40	0.82	1.48	0.179
50	6	3.5	12.2	1.75	0.732	1.37	0.168
10	8	12.7	35.7	1.27	2.86	1.63	0.197
20	8	10.1	27.6	2.02	2.21	1.56	0.189
30	8	9.3	17.7	2.79	1.42	1.40	0.172
40	8	8.0	11.1	3.20	0.89	1.32	0.162
50	8	3.3	9.3	1.65	0.74	1.21	0.147
10	10	2.6	11.0	0.26	1.10	1.54	0.187
20	10	2.5	9.3	0.50	0.93	1.42	0.174
30	10	2.4	8.7	0.72	0.87	1.21	0.147
40	10	2.2	8.5	0.88	0.85	1.11	0.133
50	10	1.6	7.7	0.80	0.77	0.84	0.090

levels of 10 mg/L and 2 mg/L. In the dye–Cd(II) binary system, the dye bioaccumulation % exhibited a larger decrease in the presence of Cd(II) for each concentration of Cd(II) that was tested compared to the dye–Pb(II) system. This result supports higher competition kinetics for Cd(II). At the minimum concentration levels for Cd(II) and dye, the biomass was 1.97 g/L and the specific growth rate was 0.228 h^{-1}, which are higher than in the dye–Pb(II) system. This result indicates that toxicity was reduced in the dye–Cd(II) system compared to the dye–Pb(II) system.

3.5. Kinetics in a single system

In the absence of dye and heavy metals, the value of μ_m and K_S for *C. tropicalis* was measured to be 0.322 h^{-1} and 0.251 g/L, respectively, by the Monod equation and linear regression. The inhibitory effects of the toxic components (dye and heavy metals) were fitted to competitive, non-competitive and uncompetitive inhibition models to characterise the inhibition kinetics on *C. tropicalis*. The inhibition constants and μ_m for the dye and heavy metals were estimated from Lineweaver–Burk plots (Figs. 2–4). Table 3 shows the values obtained using competitive, non-competitive and uncompetitive model parameters. At higher concentration levels, the inhibition constants decreased, which indicated higher toxicity. K_S values increased at higher concentration levels, thereby favouring a competitive inhibition model in the present study [26]. In the non-competitive and uncompetitive inhibition models, the K_S values should have decreased [19,26], which was not favoured in the present study. These data also indicate that Pb(II) and dye exhibit similar toxicity levels, with K_I values of 369.4 mg/L

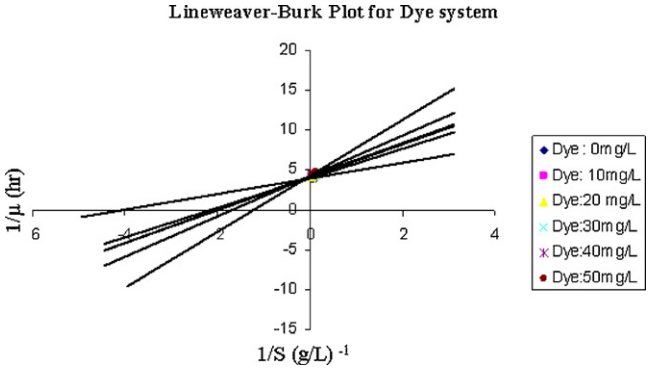

Fig. 2. Lineweaver–Burk plot for dye bioaccumulation in a single system.

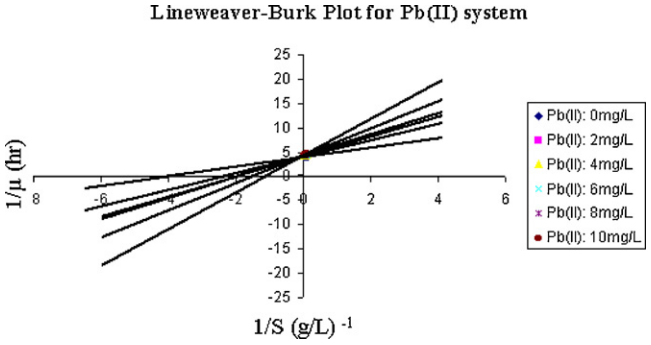

Fig. 3. Lineweaver–Burk plot for Pb(II) bioaccumulation in a single system.

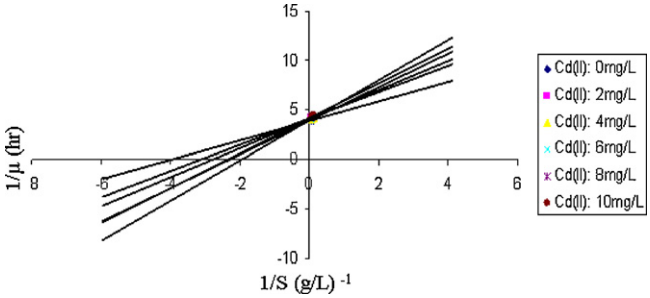

Fig. 4. Lineweaver–Burk plot for Cd(II) bioaccumulation in a single system.

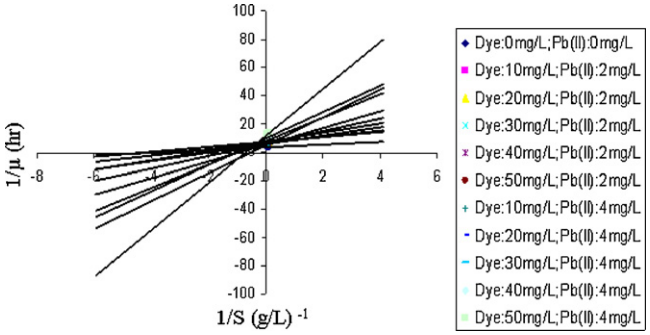

Fig. 5. Lineweaver–Burk plot for dye and Pb(II) bioaccumulation in a binary system.

at 10 mg/L of dye and 368.9 mg/L at 2 mg/L of Pb(II). These two pollutants also exhibited similar increases in their K_s values at increasing concentration levels: from 0.56 g/L to 1.04 g/L at 10 and 50 mg/L of dye concentration, respectively, and from 0.57 g/L to 0.96 g/L at 2 and 10 mg/L of Pb(II) concentrations, respectively. Cd(II) toxicity was found to be lower compared to dye and Pb(II) toxicity, as indicated by the change in the specific growth rate from 0.255 h^{-1} at 2 mg/L to 0.235 h^{-1} at 10 mg/L Cd(II) concentration. In addition, the K_I values for Cd(II) were much higher than for the Pb(II) and dye single systems, whereas the K_s values were much lower compared to the other two single systems at all concentrations.

3.6. Kinetics in a binary system

3.6.1. Dye–Pb(II) system

The toxicity studies on *C. tropicalis* in the dye–Pb(II) binary system were analysed by competitive, non-competitive and uncompetitive inhibition models using the Lineweaver–Burk plot (Fig. 5). The maximum specific growth rates decreased from 0.208 h^{-1} at 10 mg/L dye and 2 mg/L Pb(II) to 0.011 h^{-1} at 50 mg/L dye and 10 mg/L Pb(II), as shown in Table 4. Toxicity increased with an increase in concentration for each set of experiments, which was also demonstrated by an increase in the K_s values from 2.03 g/L at the lowest concentration of dye and Pb(II) to 2.72 g/L at the maximum concentration of dye and Pb(II). $K'_{s,app}$ values were calculated from the K_s values (Eq. (5)), and they demonstrated an increasing trend, indicating that the competitive inhibitory model was more favourable compared to the non-competitive and uncompetitive inhibitory models.

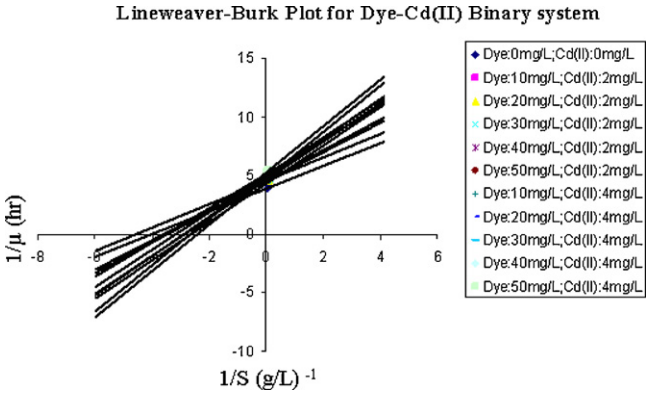

Fig. 6. Lineweaver–Burk plot for dye and Cd (II) bioaccumulation in a binary system.

3.6.2. Dye–Cd(II) system

The toxicity studies on *C. tropicalis* in the dye–Cd(II) binary system was analysed by fitting to the competitive, non-competitive and uncompetitive inhibition models using the Lineweaver–Burk plot (Fig. 6). The maximum specific growth rate decreased from 0.231 h^{-1} at 10 mg/L dye and 2 mg/L Cd(II) to 0.110 h^{-1} at 50 mg/L dye and 10 mg/L Cd(II), as shown in Table 5. Toxicity increased with an increase in concentration for each set of experiments, which was also demonstrated by an increase in the K_s values from 0.62 g/L at the lowest concentration of dye and Cd(II) to 1.13 g/L at maximum concentration of dye and Cd(II). $K'_{s,app}$ values were calculated from the K_s values (Eq. (5)), and they exhibited an increasing trend, which indicated that the competitive inhibitory

Table 3
Inhibition model parameters for Basic Violet 3, Pb(II) and Cd(II) in single system.

C_0	Competitive			Non-competitive			Uncompetitive		
	μ_m (h^{-1})	K_s (g/L)	K_I (mg/L)	μ_m (h^{-1})	K_s (g/L)	K_I (mg/L)	μ_m (h^{-1})	K_s (g/L)	K_I (mg/L)
Dye									
10	0.252	0.56	369.4	0.252	0.58	369.3	0.252	0.59	368.4
20	0.247	0.66	365.2	0.247	0.63	365.5	0.247	0.62	364.2
30	0.239	0.82	363.9	0.239	0.76	364.3	0.239	0.74	363.7
40	0.235	0.99	349.0	0.235	0.89	348.9	0.235	0.87	347.7
50	0.234	1.04	342.1	0.234	0.91	343.3	0.234	0.92	342.0
Pb(II)									
2	0.252	0.57	368.9	0.251	0.57	369.1	0.252	0.56	369.4
4	0.247	0.65	366.4	0.247	0.64	366.7	0.247	0.67	364.7
6	0.238	0.79	363.2	0.238	0.78	363.5	0.238	0.79	363.3
8	0.235	0.82	347.9	0.235	0.80	347.8	0.235	0.82	346.1
10	0.234	0.96	343.5	0.233	0.93	342.7	0.234	0.91	343.2
Cd(II)									
2	0.255	0.53	496.3	0.252	0.53	496.2	0.255	0.52	495.7
4	0.250	0.55	493.5	0.250	0.55	493.1	0.250	0.54	493.3
6	0.244	0.60	389.2	0.244	0.59	387.4	0.244	0.58	386.2
8	0.241	0.63	385.6	0.241	0.62	384.3	0.241	0.63	383.9
10	0.235	0.75	381.3	0.235	0.73	381.6	0.235	0.74	380.5

Table 4
Inhibition model parameters for Basic Violet 3 and Pb(II) in binary system.

C_0 dye	$C_{0Pb(II)}$	Competitive			Non-competitive		Uncompetitive	
		μ_m (h^{-1})	K_s (g/L)	K_{sapp} (g/L)	μ_m (h^{-1})	K_s (g/L)	μ_m (h^{-1})	K_s (g/L)
10	2	0.208	2.03	2.09	0.214	2.16	0.215	2.17
20	2	0.192	2.06	2.18	0.204	2.32	0.204	2.34
30	2	0.183	2.09	2.27	0.199	2.47	0.198	2.47
40	2	0.179	2.13	2.39	0.196	2.67	0.195	2.65
50	2	0.160	2.15	2.47	0.184	2.85	0.186	2.84
10	4	0.159	2.17	2.25	0.165	2.34	0.164	2.35
20	4	0.153	2.18	2.32	0.163	2.48	0.163	2.49
30	4	0.135	2.20	2.41	0.148	2.63	0.147	2.64
40	4	0.115	2.23	2.51	0.129	2.83	0.128	2.85
50	4	0.098	2.27	2.63	0.113	3.04	0.114	3.06
10	6	0.135	2.29	2.39	0.141	2.49	0.140	2.48
20	6	0.114	2.32	2.49	0.122	2.66	0.123	2.67
30	6	0.094	2.37	2.60	0.103	2.86	0.103	2.88
40	6	0.078	2.39	2.70	0.088	3.06	0.087	3.03
50	6	0.053	2.42	2.81	0.062	3.27	0.063	3.28
10	8	0.113	2.45	2.57	0.119	2.70	0.118	2.69
20	8	0.090	2.47	2.66	0.097	2.87	0.095	2.86
30	8	0.068	2.51	2.77	0.075	3.07	0.075	3.05
40	8	0.046	2.53	2.87	0.052	3.27	0.052	3.27
50	8	0.018	2.57	3.00	0.021	3.51	0.020	3.50
10	10	0.089	2.59	2.74	0.094	2.89	0.093	2.87
20	10	0.074	2.62	2.84	0.080	3.08	0.076	3.06
30	10	0.039	2.67	2.97	0.043	3.30	0.043	3.27
40	10	0.012	2.69	3.08	0.014	3.52	0.013	3.51
50	10	0.011	2.72	3.20	0.013	3.75	0.011	3.77

Table 5
Inhibition model parameters for Basic Violet 3 and Cd(II) in binary system.

C_0 dye	$C_{0Cd(II)}$	Competitive			Non-competitive		Uncompetitive	
		μ_m (h^{-1})	K_s (g/L)	K_{sapp} (g/L)	μ_m (h^{-1})	K_s (g/L)	μ_m (h^{-1})	K_s (g/L)
10	2	0.231	0.62	0.64	0.238	0.66	0.239	0.65
20	2	0.224	0.64	0.68	0.237	0.72	0.230	0.70
30	2	0.219	0.67	0.73	0.236	0.79	0.227	0.73
40	2	0.211	0.69	0.77	0.236	0.86	0.225	0.75
50	2	0.199	0.71	0.82	0.228	0.94	0.223	0.79
10	4	0.219	0.73	0.76	0.226	0.78	0.222	0.73
20	4	0.215	0.75	0.80	0.224	0.83	0.221	0.75
30	4	0.197	0.77	0.84	0.214	0.91	0.215	0.90
40	4	0.195	0.79	0.89	0.212	0.96	0.213	0.92
50	4	0.189	0.80	0.92	0.211	1.03	0.211	0.99
10	6	0.214	0.82	0.85	0.222	0.89	0.210	1.03
20	6	0.201	0.84	0.90	0.216	0.96	0.209	1.07
30	6	0.195	0.85	0.93	0.214	1.02	0.206	1.13
40	6	0.184	0.87	0.98	0.207	1.11	0.205	1.17
50	6	0.172	0.89	1.03	0.200	1.20	0.204	1.19
10	8	0.200	0.90	0.94	0.209	0.99	0.202	1.25
20	8	0.193	0.93	1.00	0.207	1.08	0.197	1.27
30	8	0.176	0.94	1.04	0.194	1.14	0.196	1.32
40	8	0.165	0.96	1.09	0.187	1.23	0.194	1.37
50	8	0.151	0.97	1.13	0.176	1.32	0.193	1.39
10	10	0.190	0.99	1.04	0.200	1.09	0.191	1.43
20	10	0.176	1.06	1.15	0.191	1.24	0.187	1.45
30	10	0.151	1.09	1.21	0.167	1.34	0.184	1.47
40	10	0.136	1.11	1.27	0.156	1.45	0.163	1.49
50	10	0.110	1.13	1.30	0.129	1.52	0.132	1.56

model was most favourable. The K_s values in the dye–Cd(II) system were much lower than in the dye–Pb(II) system, indicating that the dye–Cd(II) system was less toxic than the dye–Pb(II) system.

3.7. Application of RSM

Response surface methodology was used to evaluate the binary effects of Basic Violet 3 and heavy metals, viz., Pb(II) and Cd(II), as

Table 6
Comparison of values of Basic Violet 3 and Pb(II) bioaccumulation % experimentally obtained and predicted from RSM.

Run	*A*	*B*	Bioaccumulation %			
			C dye (-exp)	*D* Pb(II) (-exp)	Pred – R_1	Pred – R_2
1	30	6	23 ± 0.01	23.2 ± 0.02	23	23.2
2	30	6	23 ± 0.01	23.2 ± 0.02	23	23.2
3	30	0.34	40 ± 0.04	40.2 ± 0.01	38.2	39.0
4	58.28427	6	10.1 ± 0.02	11.0 ± 0.05	10.0	10.9
5	10	10	14.1 ± 0.04	13.9 ± 0.03	13.9	13.4
6	1.715729	6	36.1 ± 0.02	34.9 ± 0.06	36.0	35.5
7	30	6	23.0 ± 0.01	23.2 ± 0.03	23.0	23.2
8	50	2	16.8 ± 0.03	17.6 ± 0.02	17.1	18.3
9	50	10	10.8 ± 0.04	10.9 ± 0.01	10.6	10.6
10	30	6	23.0 ± 0.01	23.2 ± 0.01	23.0	23.2
11	10	2	49.5 ± 0.01	49.6 ± 0.05	50.5	50.5
12	30	6	23.0 ± 0.02	23.2 ± 0.01	23.0	23.2
13	30	11.65685	7.7 ± 0.03	7.2 ± 0.03	7.8	7.4

well as to optimise the relative dose of these toxic components. A central composite design was employed to analyse the factors, which consisted of 13 runs performed in duplicate for each binary system.

3.7.1. Analysis of the effects of factors, viz., dye and Pb(II), using the central composite design

The effects of two factors, i.e., Basic Violet 3 (denoted as A) and Pb(II) (denoted as B), on two responses, viz., Basic Violet 3 (B.V.) bioaccumulation % (denoted as C) and Pb(II) bioaccumulation % (denoted as D), were analysed and are shown in Table 6. Two numerical correlations were used to estimate the responses of dye and Pb(II) bioaccumulation % and are given by the following equation:

$$\text{B.V. bioaccumulation}\,\% = 23 - 9.18A - 10.79B + 7.53AB - 0.162A^2 + 0.21B^2 \quad (8)$$

This equation can be modified by considering the significance of the factors in the following equations:

$$\text{B.V. bioaccumulation}\,\% = 23 - 9.18A - 10.79\,B + 7.53AB \quad (9)$$

$$\text{Pb(II) bioaccumulation}\,\% = 23.2 - 8.72A - 11.22B + 7.35AB - 0.16A^2 - 0.08B^2 \quad (10)$$

Eq. (10) can be modified as follows:

$$\text{Pb(II) bioaccumulation}\,\% = 23.2 - 8.72A - 11.22B + 7.35AB \quad (11)$$

The predicted responses were calculated using these equations, as shown in Table 6. The data obtained from the above equations were significant, as verified by the *F*-test ANOVA (Tables 7 and 8). Significance of each coefficient for dye and Pb(II) bioaccumulation was determined by calculating *p*-values, as listed in Tables 7 and 8.

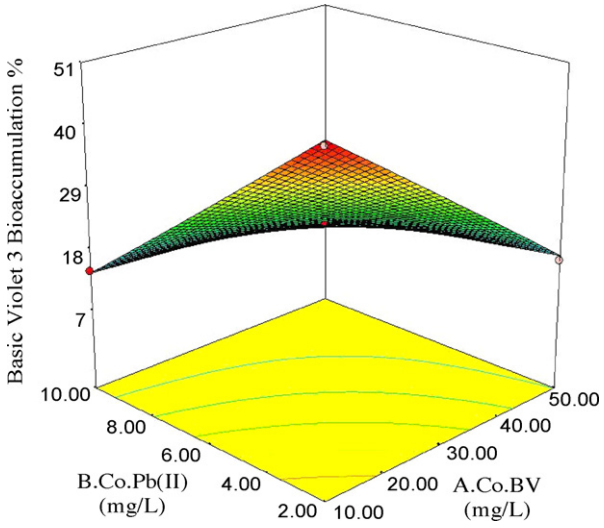

Fig. 7. Effect of Pb(II) ions on dye bioaccumulation by *C. tropicalis* in a binary system.

In the dye–Pb(II) system, the linear effect of coefficients *A* and *B*, i.e., Basic Violet 3 ($p < 0.0001$) and Pb(II) ($p < 0.0001$), and the interaction effect AB ($p < 0.0001$) were significant for both B.V. bioaccumulation % and Pb(II) bioaccumulation %. The ANOVA for the response surface model gave an *F*-value of 568.06 for B.V. bioaccumulation % (Table 7) and 384.073 for Pb(II) bioaccumulation % (Table 8). The R^2 value was 0.998, demonstrating a probability < 0.0001 for both dye and Pb(II) bioaccumulation %. The coefficient of variation was 3.489% for B.V. bioaccumulation % (Table 7) and 4.237% for Pb(II) bioaccumulation % (Table 8), indicating that the model was highly significant and that the experiments done in replicates were highly accurate and reliable. Experimen-

Table 7
Analysis of variance (ANOVA) for response surface quadratic model (dye bioaccumulation %).

Source	Sum of squares	df	Mean square	*F*-Value	*p*-Value Prob > *F*
Model	1834.480	5	366.897	568.060	<0.0001 significant
A – BV	674.722	1	674.722	1044.650	<0.0001
B – Pb(II)	932.676	1	932.676	1444.030	<0.0001
AB	226.503	1	226.502	350.690	<0.0001
A^2	0.182	1	0.182	0.283	0.6117
B^2	0.311	1	0.311	0.481	0.5103
Residual	4.521	7	0.646		
Lack of fit	4.521	3	1.507		

C.V.% 3.489; R^2 0.998; adj R^2 0.996; pred. R^2 0.982; adeq. prec. 77.656.

Table 8
Analysis of variance (ANOVA) for response surface quadratic model (Pb(II) bioaccumulation %).

Source	Sum of squares	df	Mean square	*F*-Value	*p*-Value Prob > *F*
Model	1832.552	5	365.511	384.073	<0.0001 significant
A – BV	608.999	1	608.999	638.182	<0.0001
B – Pb(II)	1007.272	1	1007.272	1055.540	<0.0001
AB	216.090	1	216.090	226.445	<0.0001
A^2	0.169	1	0.169	0.177	0.6869
B^2 0.047	1	0.047	0.0496	0.8301	
Residual	6.680	7	0.954		
Lack of fit	6.680	3	2.227		

C.V. % 4.237; R^2 0.996; adj R^2 0.994; pred. R^2 0.974; adeq. prec. 64.925.

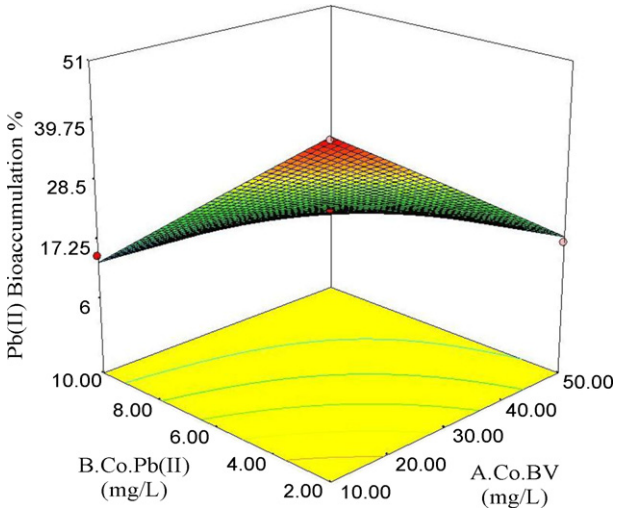

Fig. 8. Effect of dye cations on bioaccumulation of Pb(II) by *C. tropicalis* in a binary system.

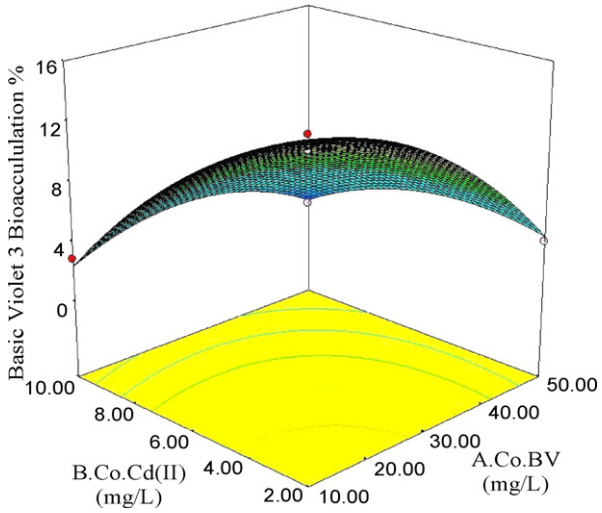

Fig. 9. Effect of Cd(II) ions on dye bioaccumulation by *C. tropicalis* in a binary system.

tal and predicted values for B.V. and Pb(II) bioaccumulation % were within 4.5% and 6.6%, respectively.

Three-dimensional mesh diagrams (Figs. 7 and 8) demonstrate that both Basic Violet and Pb(II) bioaccumulation % decreased with an increase in concentration of both toxic component, and the level of decrease was similar for both the pollutants, indicating an equal degree of competition from both dye and Pb(II) on *C. tropicalis* cells.

3.7.2. Analysis of the effects of factors, viz., dye and Cd(II), using the central composite design

The effects of two factors, i.e., Basic Violet 3 (denoted as *E*) and Cd(II) (denoted as *F*), on two responses, viz., Basic Violet 3 bioaccumulation % (denoted as *G*) and Cd(II) bioaccumulation % (denoted as *H*), were analysed and are shown in Table 9. Two numerical correlations were used to estimate the responses of dye and Cd(II) bioaccumulation % and are given by the following equations:

$$\text{B.V. bioaccumulation}\,\% = 10.2 - 2.94E - 3.96F + 2.58EF - 2.33E^2 - 1.85F^2 \quad (12)$$

$$\text{Cd(II) bioaccumulation}\,\% = 20.5 - 12.03E - 13.55F + 10.3EF + 0.89E^2 + 1.89F^2 \quad (13)$$

The predicted responses were calculated using these equations, as shown in Table 9.

Table 9
Comparison of values of Basic Violet 3 and Cd(II) bioaccumulation % experimentally obtained and predicted from RSM.

Run	*E*	*F*	Bioaccumulation%			
			G dye (-exp)	*H* Cd(II) (-exp)	Pred – R_1	Pred – R_2
1	30	6	10.2 ± 0.02	20.5 ± 0.01	10.2	20.5
2	10	2	15.9 ± 0.02	55.0 ± 0.03	15.5	53.7
3	30	6	10.2 ± 0.03	20.5 ± 0.02	10.2	20.5
4	50	10	1.6 ± 0.05	7.7 ± 0.04	1.6	7.9
5	30	6	10.2 ± 0.03	20.5 ± 0.01	10.2	20.5
6	30	0.343146	12.1 ± 0.06	42.2 ± 0.03	12.1	43.4
7	50	2	4.4 ± 0.04	15.4 ± 0.01	4.5	14.5
8	58.28427	6	1.5 ± 0.01	17.6 ± 0.05	1.5	5.3
9	10	10	2.6 ± 0.04	11.0 ± 0.04	2.5	11.5
10	30	6	10.2 ± 0.01	20.5 ± 0.03	10.2	20.5
11	1.715729	6	9.6 ± 0.06	39.3 ± 0.04	9.7	39.2
12	30	11.65685	0.87 ± 0.03	5.3 ± 0.01	0.9	5.1
13	30	6	10.2 ± 0.03	20.5 ± 0.01	10.2	20.5

Table 10
Analysis of variance (ANOVA) for response surface quadratic model dye bioaccumulation (%).

Source	Sum of squares	df	Mean square	*F*-Value	*p*-Value Prob > *F*
Model	275.308	5	55.062	310.115	<0.0001 significant
E – BV	68.928	1	68.928	388.210	<0.0001
F – Cd(II)	125.346	1	125.346	705.965	<0.0001
EF	26.523	1	26.522	149.379	<0.0001
E^2	37.625	1	37.625	211.907	<0.0001
F^2	23.760	1	23.760	133.822	<0.0001
Residual	1.243	7	0.178		
Lack of fit	1.243	3	0.414		

C.V.% 5.521; R^2 0.996; adj R^2 0.992; pred. R^2 0.968; adeq. prec. 50.963.

Table 11
Analysis of variance (ANOVA) for response surface quadratic model for Cd(II) bioaccumulation %.

Source	Sum of squares	df	Mean square	*F*-Value	*p*-Value Prob > *F*
Model	3077.467	5	615.494	737.501	<0.0001 significant
E – BV	1157.399	1	1157.399	1386.826	<0.0001
F – Cd (II)	1468.014	1	1468.014	1759.014	<0.0001
EF	424.360	1	424.360	508.479	<0.0001
E^2	5.479	1	5.479	6.566	0.0374
F^2	24.784	1	24.739	29.697	0.0010
Residual	5.841	7	0.834		
Lack of fit	5.842	3	1.947		

C.V.% 4.113; R^2 0.998; adj R^2 0.997; pred. R^2 0.986; adeq. prec. 87.059.

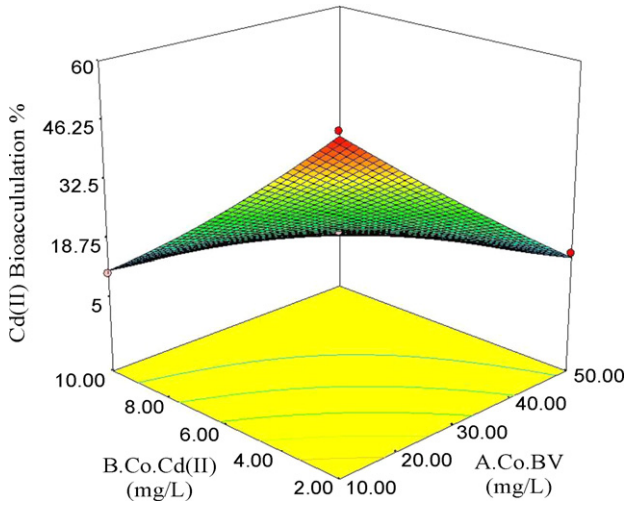

Fig. 10. Effect of dye cations on bioaccumulation of Cd(II) by *C. tropicalis* in a binary system.

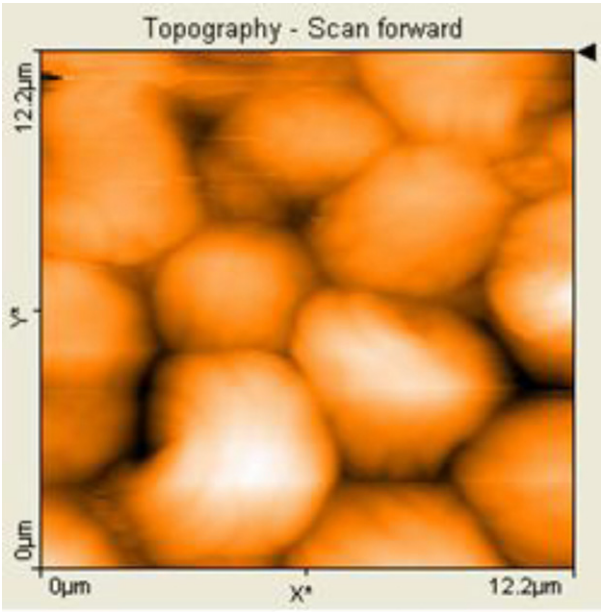

Fig. 11. AFM image of *C. tropicalis* cells grown in sugarcane bagasse extract medium without dye and heavy metals.

The data obtained from the above equations were significant, as verified by the *F*-test ANOVA (Tables 10 and 11). Significance of each coefficient for both dye bioaccumulation and Cd(II) bioaccumulation was determined by calculating *p*-values, as listed in Tables 10 and 11.

In the dye–Cd(II) system, the linear effect of coefficients *E* and *F*, i.e., Basic Violet ($p < 0.0001$) and Cd(II) ($p < 0.0001$), the interaction effect EF for both dye and Cd(II) bioaccumulation % ($p < 0.0001$), the quadratic terms E^2 ($p < 0.0001$) and F^2 ($p < 0.0001$) in the case of dye bioaccumulation % and the E^2 (*p*-value of 0.0374) and F^2 (*p*-value of 0.001) in the case of Cd(II) bioaccumulation % all demonstrated statistical significance. The ANOVA for the response surface model gave an *F*-value of 310.115 for B.V. bioaccumulation % (Table 10) and 737.501 for Cd(II) bioaccumulation % (Table 11). The R^2 value was 0.99, demonstrating a probability < 0.0001 for both dye and Cd(II) bioaccumulation %. The coefficient of variation was 5.521% for B.V. bioaccumulation % and 4.113% for Cd(II) bioaccumulation %, indicating that the model is highly significant and the experiments (done in replicates) are highly accurate and reliable. Experimental and predicted values for B.V. and Cd(II) bioaccumulation % were within 3.9% and 5.8%, respectively.

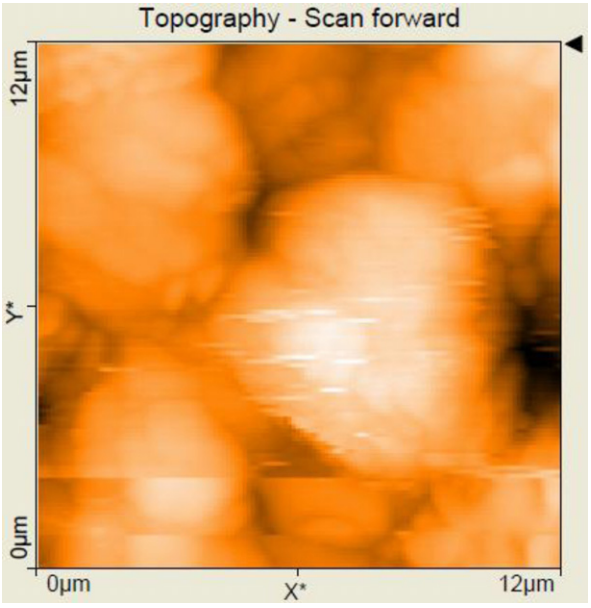

Fig. 12. AFM image of *C. tropicalis* cells grown in sugarcane bagasse extract medium containing dye cations.

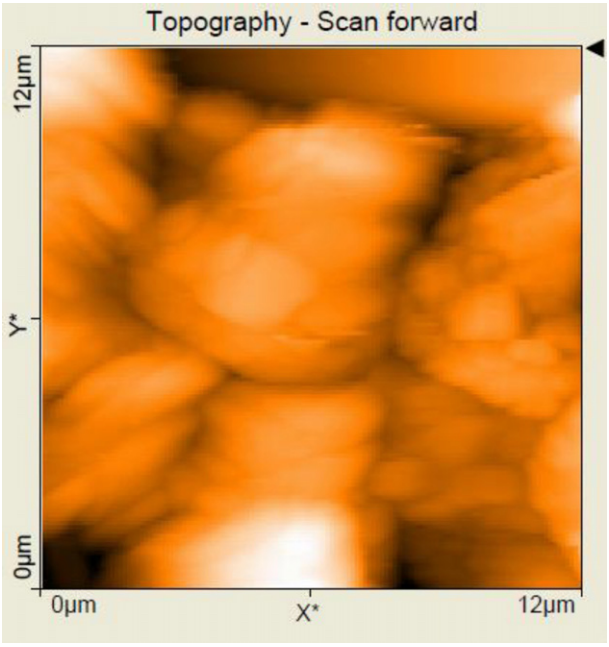

Fig. 13. AFM image of *C. tropicalis* cells grown in sugarcane bagasse extract medium containing Pb(II) ions.

Three-dimensional mesh diagrams (Figs. 9 and 10) demonstrate that both Basic Violet 3 and Cd(II) bioaccumulation % decreased with increased pollutant concentration levels, but the level of decrease for dye bioaccumulation was much higher in the presence of Cd(II) than the decrease in Cd(II) bioaccumulation in the presence of the dye, thereby indicating that the dye exhibited a higher level of competition in the presence of Cd(II).

3.8. AFM analysis

Cell morphologies of yeast before and after the bioaccumulation of the dye and Pb(II) are shown in Figs. 11–13, respectively. As

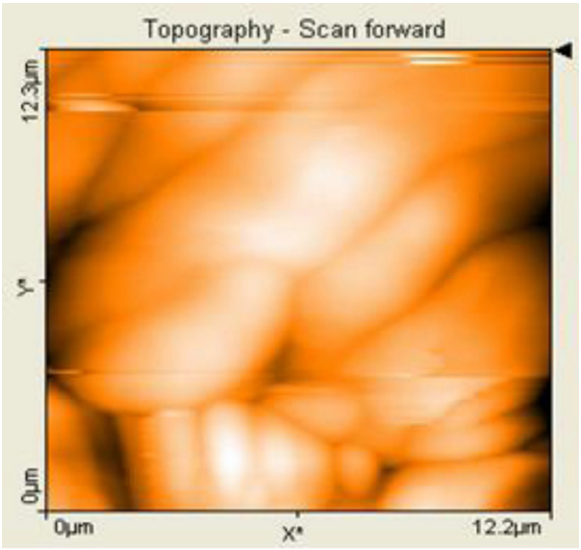

Fig. 14. AFM image of *C. tropicalis* cells grown in sugarcane bagasse extract medium containing both dye and Pb(II).

illustrated in Fig. 11, the native cell surface was smooth, full and covered with thick secretions that were mostly extracellular, such as polysaccharide, protein and amide secretions [27]. After dye and Pb(II) bioaccumulation, organic crystals were observed that formed as extracellular secretions that were bound to dye and Pb(II) in the chelating centre (Figs. 12 and 13). These crystals were attached to the cell surface and aggregated with each other, leading to a rougher surface morphology. Fig. 14 demonstrates the toxic effects of both dye and Pb(II) on *C. tropicalis* in the binary system, which resulted in cell clumping and caused contact inhibition and irregular shapes.

4. Conclusions

The results obtained in this study indicate that the growing yeast *C. tropicalis* was capable of accumulating Basic Violet 3 and the heavy metals Pb(II) and Cd(II) both separately and in combination in a batch process using sugarcane bagasse extract as an inexpensive growth medium. Maximum uptake was achieved in the absence of other pollutants and the individual uptake of each pollutant in a binary mixture was affected by the concentration and composition of the other pollutant. The presence of Pb(II) together with Basic Violet 3 caused maximum toxicity in *C. tropicalis*. RSM provided statistically reliable results to determine the optimum conditions for maximising the removal of Pb(II), Cd(II) and Basic Violet 3 by *C. tropicalis* bioaccumulation.

References

[1] P. Nigam, G. Armour, I.M. Banat, D. Singh, R. Marchant, Physical removal of textile dyes from effluents and solid-state fermentation of dye adsorbed agricultural residues, Bioresour. Technol. 72 (2000) 219–226.
[2] J.Y. Farah, N.S. El- Gendy, L.A. Farahat, Biosorption of Astrazone Blue basic dye from an aqueous solution using dried biomass of bakers yeast, J. Hazard. Mater. 148 (2007) 402–408.
[3] S.V. Mohan, N.C. Rao, P.N. Sarma, Simulated acid azo dye (Acid black 210) wastewater treatment by periodic discontinuous batch mode operation under anoxic-aerobic-anoxic microenvironment conditions, Ecol. Eng. 31 (2007) 242–250.
[4] E. Lesage, C. Mundia, D.P.L. Rousseau, A.M.K. Van de Moortel, G. Du Laing, E. Meers, F.M.G. Tack, N. De Pauw, M.G. Verloo, Sorption of Co, Cu, Ni, and Zn from industrial effluents by the submerged aquatic macrophyte *Myriophyllum spicatum* L., Ecol. Eng. 30 (2007) 320–325.
[5] A. Sari, M. Tuzen, Removal of mercury(II) from aqueous solution using moss (*Drepanocladus revolvens*) biomass: equilibrium, thermodynamic and kinetic studies, J. Hazard. Mater. 171 (2009) 500–507.

[6] M. Tuzen, A. Sari, D. Mendil, M. Soylak, Biosorptive removal of mercury(II) from aqueous solution using lichen (*Xanthoparmelia conspersa*) biomass: kinetic and equilibrium studies, J. Hazard. Mater. 169 (2009) 263–270.
[7] I. Campbell, Culture, storage, isolation and identification of yeasts, in: I. Campbell, J.H. Duffus (Eds.), Yeast: A Practical Approach, IRL Press, UK, 1988.
[8] G. Donmez, Z. Aksu, The effect of Cu(II) ions on the growth and bioaccumulation properties of some yeasts, Process Biochem. 35 (1999) 135–142.
[9] Z. Aksu, Reactive dye bioaccumulation by *Saccharomyces cerevisiae*, Process Biochem. 38 (2003) 1437–1444.
[10] G. Donmez, Bioaccumulation of the reactive textile dyes by *Candida tropicalis* growing in molasses medium, Enzyme Microb. Technol. 30 (2002) 363–366.
[11] Z. Aksu, G. Donmez, Combined effects of molasses sucrose and reactive dye on the growth and dye bioaccumulation properties of *Candida tropicalis*, Process Biochem. 40 (2005) 2443–2454.
[12] I.K. Kapdan, F. Kargi, G. Mcmullan, R. Marchant, Effect of environmental conditions on biological decolorization of textile dyestuff by *C. versicolor*, Enzyme Microb. Technol. 26 (2000) 381–387.
[13] N. Hatvani, I. Mecs, Effect of certain heavy metals on the growth, dye decolorization, and enzyme activity of *Lentinus edodes*, Ecotoxicol. Environ. Safety 55 (2003) 199–203.
[14] S. Sadettin, G. Donmez, Simultaneous bioaccumulation of reactive dye and chromium (VI) by using thermophil *Phormidium* sp., Enzyme Microb. Technol. 41 (2007) 175–180.
[15] Z. Aksu, N.K. Kilic, S. Ertugrul, G. Donmez, Inhibitory effects of chromium (VI) and Remmazol Black B on chromium (VI) and dyestuffs removals by *Tremates versicolor*, Enzyme Microb. Technol. 40 (2007) 1167–1174.
[16] F. Gonen, Z. Aksu, Use of response surface methodology (RSM) in the evaluation of growth and copper (II) bioaccumulation properties of *Candida utilis* in molasses medium, J. Hazard. Mater. 154 (2008) 731–738.
[17] S. Sharma, A. Malik, S. Satya, A of response surface methodology (RSM) for optimization of nutrient supplementation for Cr(VI) removal by *Aspergillus lentulus* AML05, J. Hazard. Mater. 164 (2009) 1198–1204.
[18] K. Ravikumar, K. Pakshirajan, T. Swaminathan, K. Balu, Optimization of batch process parameters using response surface methodology for dye removal by a novel adsorbent, Chem. Eng. J. 105 (2005) 131–138.
[19] D. Das, D. Charumathi, N. Das, Combined effects of sugarcane bagasse extract and synthetic dyes on the growth and bioaccumulation properties of *Pichia fermentans* MTCC 189, J. Hazard. Mater. 183 (2010) 497–505.
[20] R.H. Myers, D.C. Montgomery, Response Surface Methodology, 2nd ed., Wiley International, 2002.
[21] M.I. Shuler, F. Kargi, Bioprocess Engineering Basic Concepts, Prentice-Hall, Englewood Cliffs, NJ, 1992.
[22] O. Acikel, Investigation of the growth kinetics and heavy metal bioaccumulation of some yeasts growing in molasses added waste water containing heavy metals, PhD thesis, Hacettepe University, Institute of Pure and Applied Science, Ankara, 2003.
[23] Z. Aksu, G. Donmez, Combined effects of sucrose and copper(II) ions on the growth and copper(II) bioaccumulation properties of *Candida* sp., J. Chem. Technol. Biotechnol. 75 (2000) 847–853.
[24] F. Gonen, Z. Aksu, Copper(II) bioaccumulation properties of the yeast *C. tropicalis*: effect of copper(II) on growth kinetics, J. Biotechnol. 131 (2007) S165–S166.
[25] F. Gonen, Z. Aksu, Single and binary dye and heavy metal bioaccumulation properties of *Candida tropicalis*: use of response surface methodology (RSM) for the estimation of removal yields, J. Hazard. Mater. (2009), doi:10.1016/j.jhazmat.2009.08.021.
[26] O. Acikel, T. Alp, A study on the inhibition kinetics of bioaccumulation of Cu(II) and Ni(II) ions using *Rhizopus delemar*, J. Hazard. Mater. 168 (2009) 1449–1458.
[27] D.Y. Zhang, J.L. Wang, X.L. Pan, Cadmium sorption by EPSs produced by anaerobic sludge under sulfate-reducing conditions, J. Hazard. Mater. 138 (2006) 589–593.